Loss of adipocyte specification and necrosis augment tumor-associated inflammation

Marek Wagner,[1] Rolf Bjerkvig,[1,2] Helge Wiig,[1] and Andrew C Dudley[3,*]

[1]Department of Biomedicine; University of Bergen; Bergen, Norway; [2]Centre de Reserché Public de la Santé; Luxembourg, Luxembourg; [3]Department of Cell Biology & Physiology; Lineberger Comprehensive Cancer Center & McAllister Heart Institute; The University of North Carolina at Chapel Hill; Chapel Hill, NC USA

Most tumors are typified by a chronic, unresolved inflammatory response that potentiates angiogenesis and therefore enables tumor progression. We have determined that dysfunctional tumor-associated adipocytes contribute to tumor-associated inflammation. In three tumor models, tumor-associated adipose tissue was characterized by thin and fragile adipocyte membranes, necrosis, robust expression of the pro-inflammatory factor HMGB1, and loss of the lipid storage mediator, perilipin-1. By transmission electron microscopy, macrophages in tumor-associated adipose tissue contained lipid droplets and resembled foam cells, which are commonly observed in inflamed tissues. In vitro co-culture studies showed that tumor-associated adipose tissue conditioned-medium stimulated monocyte-to-macrophage differentiation, adhesion, spreading, and lipid uptake. Compared with normal adipose tissue, tumor-associated adipose tissue secreted 3-fold higher levels of IL-6 and IL-6 was sufficient to stimulate macrophage differentiation and adhesion. These results suggest that, in tumors, loss of adipocyte specification, necrosis, and scavenging of adipocyte debris directly activates macrophages and contributes to tumor-associated inflammation. Thus, adipocyte dysfunction may facilitate tumor progression, especially in tumors closely aligned with adipose tissue, in particular, breast cancer.

Introduction

Unlike fibroblasts, inflammatory cells, and vascular endothelial cells, adipocytes have been frequently overlooked as a significant stromal cell "compartment" in solid tumors.[1] Nevertheless, several recent studies have determined that adipocytes affect multiple processes related to tumor progression. Adipocytes may directly stimulate tumor cell survival, proliferation, and migration.[2,3] Heterotypic interactions between adipocytes and tumor cells increase radio- and chemo-resistance.[4,5] Adipocytes stimulate melanoma cell invasion by increasing expression of epithelial-to-mesenchymal (EMT) effectors while downregulating expression of E-cadherin and the metastasis suppressor, Kiss1.[6] Moreover, injection of 4T1 breast cancer cells primed with mature adipocytes increased lung metastases.[7] In ovarian cancers, which frequently metastasize to the omentum, adipocytes were shown to promote homing and growth of cancer cells.[8] Additionally, co-culture of adipocytes with cancer cells led to increased adipocyte lipolysis and β-oxidation in cancer cells.[8] It has therefore been suggested that adipocytes act as a direct energy source for tumors. Taken together, tumor-associated adipocytes may play a prevailing role in the growth of multiple tumor types, especially those which are localized near or within an adipose tissue (AT) depot.

AT also harbors numerous inflammatory cells, especially macrophages.[9] Macrophages are highly-specialized cells of the innate immune system that remove bacteria, debris, and dead or dying cells by phagocytosis. Remarkably, apoptotic cells elicit a different type of macrophage polarization compared with necrotic cells. Necrotic cells lose membrane integrity and rapidly expel their intracellular contents that contain pro-inflammatory signals including the high-mobility group box 1 protein (HMGB1). HMGB1 released into the extracellular space transduces cellular signals through RAGE (receptor for advanced glycation end products) and possibly other receptors, such as Toll-like receptor 2 (TLR2) and TLR4 expressed in macrophages. HMGB1 drives activation pathways that involve nuclear factor-κB (NFκB) leading to transcription of pro-inflammatory genes, including IL-6.[10] On the other hand, apoptotic cells, by initially maintaining their membrane integrity, may not provoke an inflammatory response.[11] For example, in advanced atherosclerotic plaques, macrophages produce pro-inflammatory mediators following ingestion of apoptotic cells undergoing secondary necrosis, but not by intact apoptotic cells.[12] Moreover, apoptotic cells can stimulate macrophages to produce anti-inflammatory mediators such as interleukin-10 (IL-10) or transforming growth factor-β (TGF-β).[11]

Macrophages and other inflammatory cells play a well-recognized role in tumor progression and metastasis.[13] While tumor- and stromal-derived chemokines and pro-inflammatory cytokines are well-known to promote macrophage recruitment and polarization, it is less certain if other stimuli can

fuel tumor-associated inflammation. We recently showed that inflamed tumor-associated AT is fibrotic, highly vascularized, and infiltrated by abundant adipose tissue macrophages (ATMs).[14,15] Here, we have further investigated the nature of adipocyte-derived chemo-attractant signals that promote and/or activate macrophages in peritumoral AT. The results show that, in tumors, adipocytes undergo phenotypic and functional alterations resulting from loss of specification, necrosis, and lipid release. Moreover, peritumoral AT harbors increased numbers of macrophages, which ingest and sequester necrotic adipocyte debris and freed lipids, coincident with increased IL-6 expression. These findings implicate adipocyte necrosis as a pathologic marker of tumor progression and, furthermore, suggest that macrophages within tumor-associated AT may be directly activated by up-take of adipocyte-derived lipid droplets.
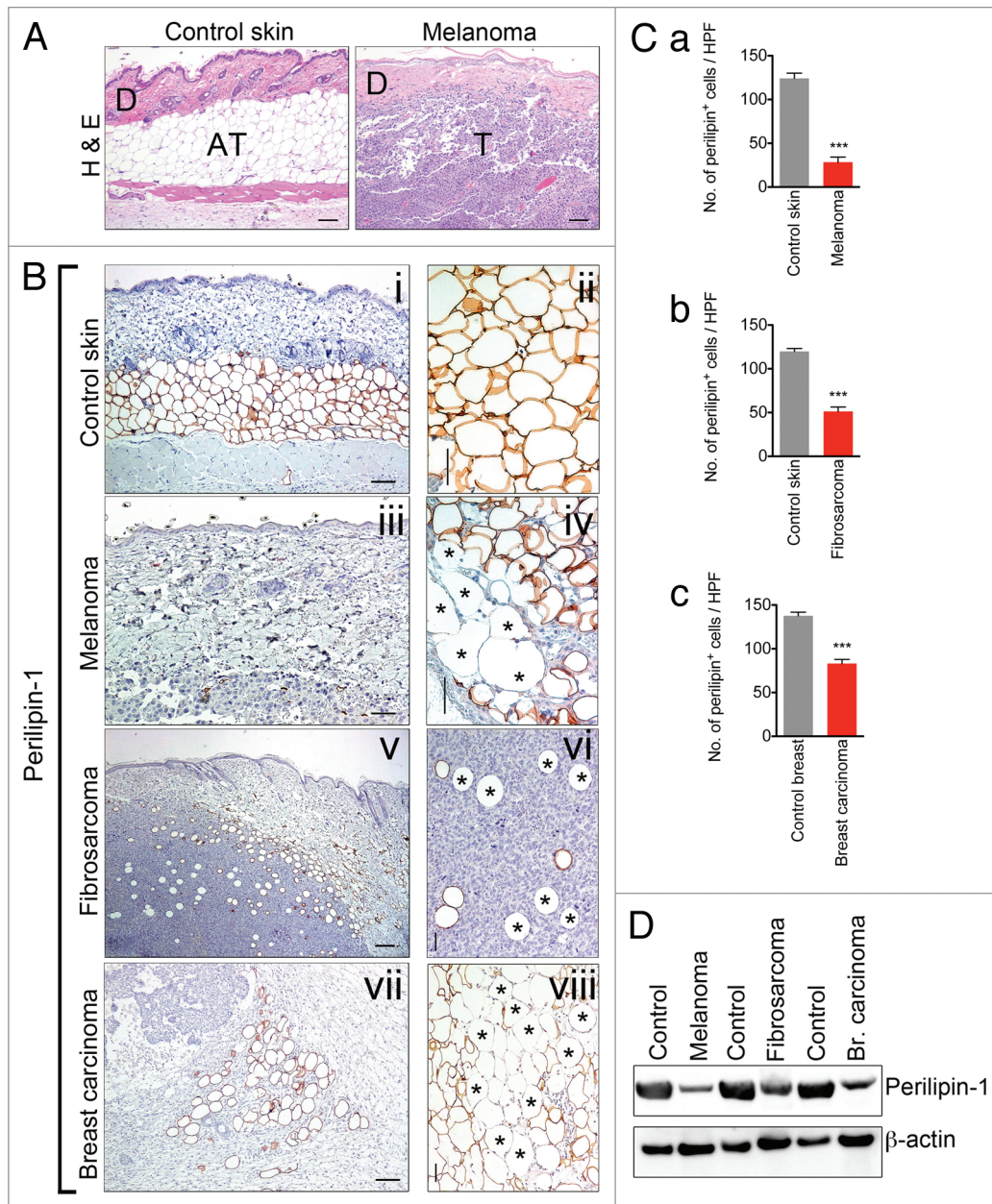
Results

Adipose tissue juxtaposed to implanted tumors is atrophied and demonstrates diminished expression of the lipid storage mediator, perilipin-1. To characterize tumor-associated AT, B16F10 melanoma and KHT-1 fibrosarcoma cells were implanted subcutaneously into immunocompetent C57BL6/J and C3H mice, respectively. C3HBA breast carcinoma cells were implanted orthotopically into the mammary fat pad of immunocompetent C3H mice. When tumors reached 2 cm in diameter, tumors and the surrounding subcutaneous connective tissues were carefully micro-dissected as previously described by us.[14] Under microscopic examination of H&E-stained sections, B16F10 tumors contained few, thin-walled, and poorly-organized adipocytes when compared with control skin (**Fig. 1A**). This observation was confirmed by staining tissues with antibodies raised against the lipid droplet-associated protein, perilipin-1. In contrast to control skin (**Fig. 1B, i and ii**), numerous "empty sleeves" of adipocytes were observed in melanoma (**Fig. 1B, iii and iv**), fibrosarcoma (**Fig. 1B, v and vi**), and breast carcinoma (**Fig. 1B, vii and viii**). Moreover, adipocytes in these sections appeared thin-walled and poorly organized. By quantifying the perilipin-1 stained areas, it was determined that the number of perilipin-1 positive adipocytes was reduced 4-fold in melanoma compared with normal skin sections whereas a 2-fold decrease in the number of perilipin-1 positive cells was observed in fibrosarcoma and breast carcinoma (**Fig. 1C, a–c**). Western blot analysis confirmed reduced protein levels of perilipin-1 in melanoma, fibrosarcoma, and breast carcinoma lysates (**Fig. 1D**). Together, these observations suggest that tumor-associated adipocytes are characterized by gross changes in morphology, loss of specification, and atrophy.

Peritumoral adipose tissue atrophy is accompanied by infiltration of HMGB1⁺ inflammatory cells and adipocyte necrosis. We have previously shown that tumor-associated AT is characterized by fibrosis, angiogenesis, and inflammation.[14] Because adipocyte membranes in tumor-associated AT appeared discontinuous with accompanying inflammatory cell infiltration, we hypothesized that tumor-associated adipocytes might also undergo necrosis which could act, in part, as a stimulus for inflammatory cell recruitment. High-mobility group box 1 protein (HMGB1)

is frequently used as a marker of necrosis in sites of sterile inflammation; thus, we stained control AT and peritumoral AT tissues with HMGB1 antibodies.[16,17] Whereas HMGB1 was predominantly localized to the nucleus in control AT, in peritumoral AT intense HMGB1 staining was observed throughout the cytoplasm of adipocytes and in both cytoplasm and nuclei of inflammatory cells (**Fig. 2A, i–iii**). Notably, HMGB1 is reported to act upstream of IL-6 expression and the HMGB1 expression pattern matched IL-6 expression in vivo (**Fig. 2A, iv–vi**).[14,18] We then assessed the number of viable, apoptotic, and necrotic cells in freshly isolated adipocytes from control and peritumoral AT using an ethidium bromide/acridine orange (EB/AO) viability stain (**Fig. 2B, a, i and ii**). Approximately 20% of adipocytes from peritumoral AT were identified as necrotic, whereas none were found from control AT (**Fig. 2B, b**). Control and peritumoral AT was then examined using transmission electron microscopy (TEM). Under TEM examination, adipocytes from control AT demonstrated the classic double-membrane structure with peripheral nuclei and a single, centralized lipid droplet (**Fig. 2C, i–iii**). On the other hand, peritumoral AT exhibited ultrastructural features of necrosis, including ruptured basal membranes, which accompanied extruded cellular debris in the extracellular space (**Fig. 2C, iv–vi**). None of the common ultrastructural features of apoptosis, such as chromatin condensation, plasma membrane blebbing, or membrane-bound apoptotic bodies with nuclear fragments were obvious in adipocytes from control or peritumoral AT. Immunohistochemical analysis of the apoptotic marker cleaved caspase-3 revealed none or occasional apoptotic adipocytes within peritumoral AT (data not shown). Taken together, these results demonstrate that adipocytes within peritumoral AT display features of necrotic cell death which is accompanied by cytoplasmic localization of HMGB1.

Peritumoral adipose tissue is enriched with lipid-laden inflammatory cells in vivo and macrophages can be induced to differentiate in response to peritumoral adipose tissue conditioned medium in vitro. Using TEM, we observed numerous lipid-laden macrophages in peritumoral AT, indicated by the presence of lipid droplets, which was also confirmed by intense expression of adipose differentiation-related protein (ADRP), a major lipid droplet protein involved in the regulation of lipid-laden macrophage or "foam cell" formation (**Fig. 3A** and data not shown).[19,20] Furthermore, isolated stromal vascular fractions (SVF) from peritumoral AT revealed an ~10-fold increase in Oil-red-O stained cells compared with control AT (**Fig. 3B, a and b**). Immunolabeling using CD11b, a marker of monocytes/macrophages, revealed that ~90% of SVF cells were CD11b positive (data not shown). Next, we co-cultured mouse monocytes with conditioned medium collected from control or peritumoral AT.[14] After exposure to conditioned medium from peritumoral AT, western blotting revealed an ~2.5-fold upregulation of CD301, a marker of alternatively activated (M2) macrophages (**Fig. 3C, a**). Incubation with peritumoral AT-conditioned medium also resulted in monocytes acquiring characteristics reminiscent of macrophages including a change in morphology from round, non-adherent cells to flattened, adherent cells (**Fig. 3C, b**). Moreover, we observed a 2-fold increase in the number of

Figure 1. Adipose tissue juxtaposed to implanted tumors is atrophied and demonstrates diminished expression of the lipid storage mediator, perilipin-1. Hematoxylin-eosin histological examination of control mouse skin, size bar = 100 μm (left panel) and mouse model of melanoma, B16F10, size bar = 100 μm (right panel), revealed atrophy of tumor-associated AT. "D" marks dermis, "AT" marks adipose tissue and "T" marks tumor (**A**). Immunohistochemical analysis of tissue sections from control mouse skin, size bar = 100 μm and 50 μm (**B, i and ii**) and peritumoral area of melanoma, size bar = 100 μm and 50 μm (**iii and iv**), fibrosarcoma, size bar = 200 μm and 50 μm (**v and vi**) and breast carcinoma, size bar = 100 μm and 50 μm (**vii and viii**) using adipocyte marker, lipid droplet-associated protein, perilipin-1. Perilipin-1 negative adipocyte-like cells are marked by an asterisk. Quantification of perilipin-1+ cells within control mouse skin (*n* = 3/group) and tumor samples (*n* = 3/group) revealed decreased numbers of perilipin-1+ cells surrounding tumors (**C, a–c**). Western blot was performed using control mouse skin and tumor samples with overlying connective tissue. Western blot results revealed decreased levels of perilipin-1 within tumor samples with overlying connective tissue when compared with skin samples (**D**). Data presented are mean values ± SEM *P < 0.05; **P < 0.01; and ***P < 0.001, the Student *t* test.

Oil-red-O positive macrophages (**Fig. 3C, c**) and an ~5-fold increase in the number of lipid droplets per individual macrophage (**Fig. 3C, d**) when peritumoral AT-CM was added. Lipid accumulation accompanied a decrease in monocyte proliferation (**Fig. 3C, e**). We previously reported that IL-6 expression was strikingly upregulated in peritumoral AT when measured using a tissue microarray.[14] Moreover, IL-6 expression was strikingly increased in peritumoral AT sections. Thus, we hypothesized that peritumoral AT-derived IL-6 might be an effector of macrophage differentiation in our in vitro assay. We first confirmed that IL-6 was present in conditioned medium from peritumoral AT using an ELISA. Compared with conditioned medium from control
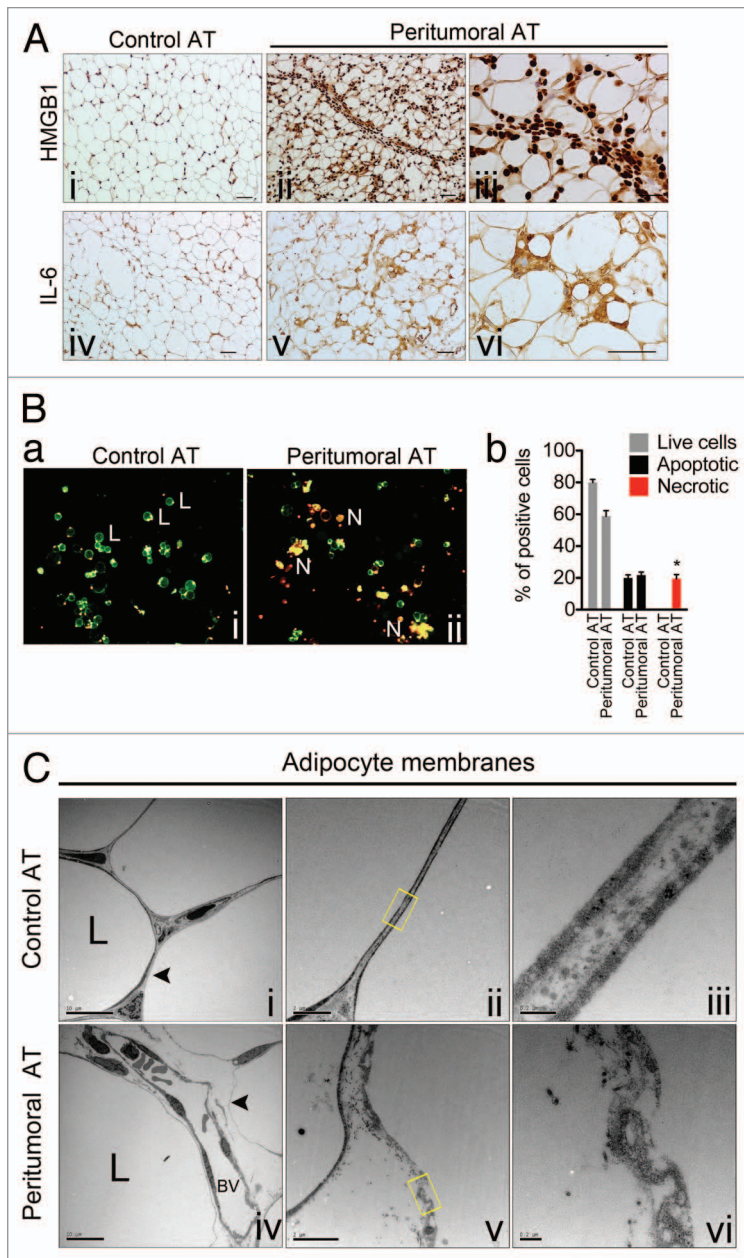
Figure 2. Peritumoral adipose tissue atrophy is accompanied by infiltration of HMGB1⁺ inflammatory cells and adipocyte necrosis. Immunohistochemical analysis for marker of necrosis, HMGB1 revealed intensive cytoplasmic staining of adipocytes from peritumoral AT as well as the presence of HMGB1⁺ inflammatory cells, size bar = 50 μm (**A, i and ii**) and size bar = 25 μm (**iii**). The HMGB1 expression pattern matched that of IL-6, size bar = 50 μm (**iv and v**) and size bar = 25 μm (**vi**). Morphology of adipocytes isolated from control and peritumoral AT and then stained using Ethidium Bromide/Acridine Orange. Live cells (L) stain green and are round with two or fewer yellow dots; apoptotic cells with intact plasma membranes stain green, are irregularly shaped, often due to membrane blebbing, and contain multiple yellow/green dots of condensed nuclei. Cells undergoing necrosis (N) stain bright orange due to the influx of ethidium bromide and contain multiple yellow/green/orange condensed nuclei (**B, a**). Quantification of live, apoptotic and necrotic cells (**b**). Electron micrograph examining adipocyte membranes in control and peritumoral AT (**C, i–vi**). Note the ruptured basal membrane and presence of cellular debris in peritumoral AT. The boxed yellow areas are magnified in (**iii and vi**). "L" marks the lipid droplet and "BV" marks a blood vessel. Data presented are mean values ± SEM *P < 0.05; **P < 0.01; and ***P < 0.001, the Student t test.

AT, we found a 3-fold increase in IL-6 levels in conditioned medium from peritumoral AT (**Fig. 3D, a**). Direct IL-6 stimulation resulted in a dose-dependent decrease in monocyte proliferation (**Fig. 3D, b**) and an increase in macrophage adhesion (**Fig. 3D, c**). Taken together, these results indicate that peritumoral AT-conditioned medium stimulates monocyte-to-macrophage differentiation and that IL-6 is a principle factor controlling this process.
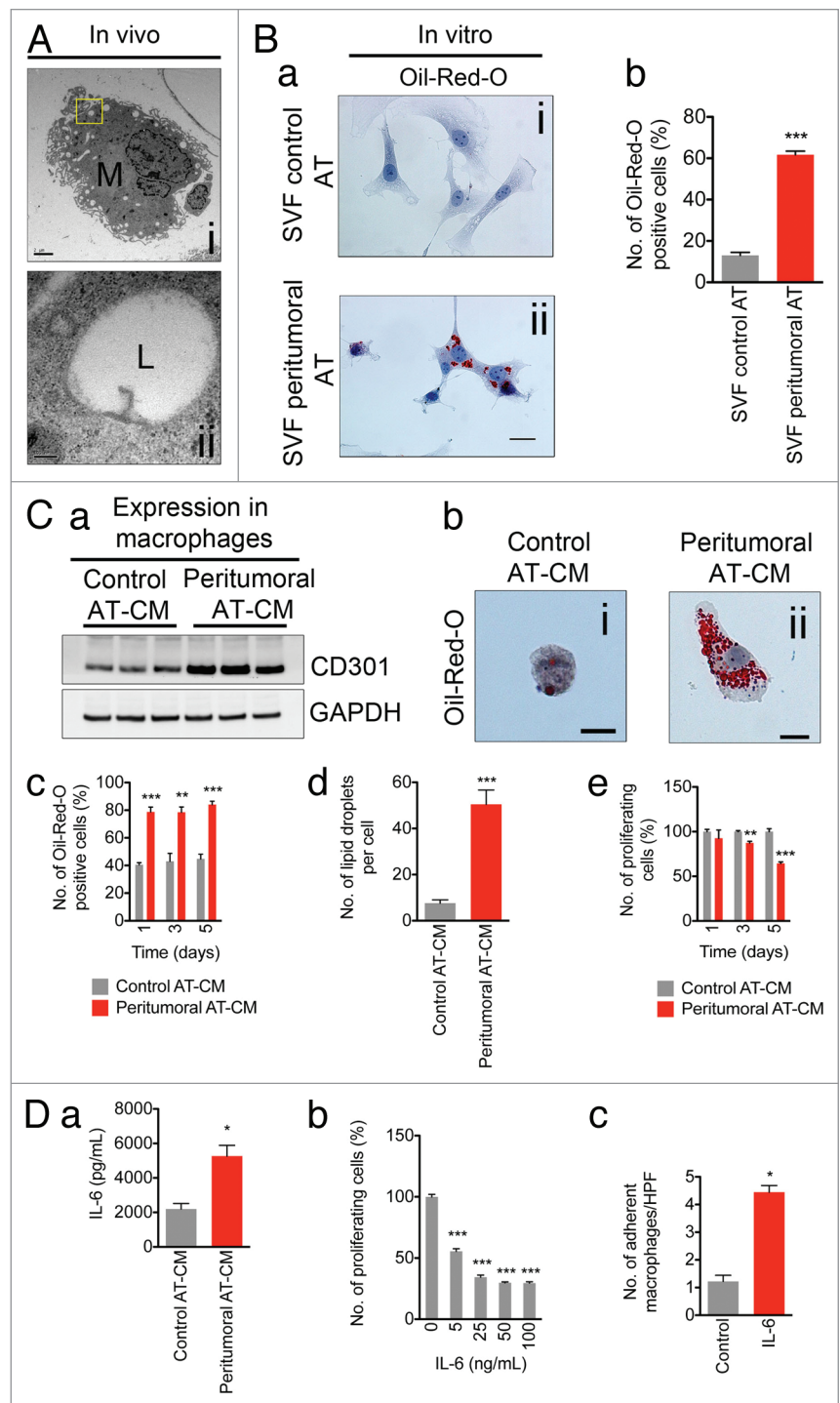
Discussion

Tumor-associated inflammation contributes to tumor development by enhancing angiogenesis, promoting metastatic spread, inducing local immunosuppression, and increasing genomic instability.[21] Chemokines and pro-inflammatory cytokines expressed by tumor cells and inflammatory cells are thought to be the predominant drivers of tumor-associated inflammation. However, the role of the adipocyte as a contributor to tumor-associated inflammation has not been well-studied. As demonstrated in our previous report, peritumoral AT exhibits extensive phenotypic changes including decreased adipocyte size, increased fibrosis, enhanced angiogenesis, and macrophage infiltration.[14] However, neither the underlying adipocyte-related effectors nor the function of macrophages localized to peritumoral AT was clear. Here, we show that adipocytes from peritumoral AT undergo necrotic cell death which may underlie the recruitment and polarization of macrophages thereby igniting a sterile inflammatory response.

It is well-established that necrotic cell death stimulates a host of inflammatory responses.[11] Necrotic death is usually triggered by physical trauma or insults leading to cellular membrane rupture and liberation of damage-associated molecular patterns (DAMPs) into the extracellular space. DAMPs are recognized by immune cells leading to the induction of sterile inflammation.[22] Among DAMPs are intracellular components, such as HMGB1, a non-histone chromatin-associated protein. Once released from necrotic cells, HMGB1 functions as a proinflammatory cytokine, binding to innate immune receptors such as receptor for glycation end products (RAGE), Toll-like receptor 2 (TLR2) and TLR4, and drives the expression of NFκB-activated cytokines such as TNF-α, IL-1β, and IL-6.[10,16] In apoptotic cells, however, HMGB1 is bound firmly to chromatin due to generalized deacetylation of histones and chromatin condensation. Thus, cells undergoing apoptosis retain HMGB1 within nuclear remnants and do not trigger an inflammatory response.[16] Apart from being passively released from necrotic cells, HMGB1 is also secreted by activated monocytes and macrophages via a non-classical vesicle-mediated secretory pathway following stimulation with various activation signals (e.g., lipopolysaccharide) and pro-inflammatory molecules (e.g., TNF-α).[23,24]

We found that tumor-associated adipocytes exhibit some of the hallmarks of necrotic cell death including membrane rupture. As necrotic death is usually triggered by physical trauma or insults, we can only speculate that rapid expansion of the tumor mass, by creating biomechanical forces, leads to distortion of fragile adipocyte cellular membranes, loss of adipocyte specification and function, and eventually cell death due to membrane rupture. Necrotic death could therefore promote macrophage recruitment and activation through release of DAMPs, such as HMGB1. It has been shown that stimulation of human monocytes with HMGB1 induces production of TNF-α, IL-1α, IL-1β, IL-1RA, IL-6, IL-8, macrophage inflammatory protein (MIP)-1α, and MIP-1β.[18] Induction of pro-inflammatory cytokine expression by HMGB1 might therefore trigger a chronic inflammatory response resulting in further inflammatory cell recruitment into peritumoral AT.

Dirat et al. has shown that adipocytes cocultivated with breast tumor cells undergo extensive phenotypic changes including lipid depletion, a decrease in adipocyte markers, and overexpression of inflammatory cytokines and proteases.[7] Thus, when in contact with tumor cells, adipocytes may "de-differentiate" to form fibroblast-like cells and perhaps contribute to the pool of tumor-associated fibroblasts that are well-known to play important roles in inflammation and fibrosis. In these same co-culture experiments, tumor cells in contact with adipocytes became more invasive and migratory indicating that adipocyte-to-tumor cell cross-talk is complimentary. Thus, both adipocyte necrosis and de-differentiation could play non-mutually exclusive roles in modifying adipocyte function. By doing so, adipocytes acquire new features and express a new repertoire of cytokines, chemokines and other factors that fuel tumor-associated inflammation. It would be interesting to determine that "fate" of tumor-associated adipocytes using lineage tracing experiments in mice to assess the temporal and spatial patterns of adipocyte differentiation. Using this model, it may be possible to correlate loss of adipocyte specification with infiltration of pro-inflammatory cells. Based on our findings and those of others, we predict that the two will go hand-in-hand and that loss of adipocyte specification

will occur early or coincide with the establishment of the desmoplastic response typical of invasive cancers.[2,3]

The ability of pro-inflammatory cells to enable tumor growth has been well-characterized in numerous mouse tumor models. Paracrine factors that initiate inflammation emanate from multiple cell types. For example, cells of the innate immune system and tumor-associated fibroblasts are thought to be the principle source of pro-inflammatory factors.[25-27] On the other hand, adipocytes have been frequently ignored as key determinants of tumor-associated inflammation. We found that addition of peritumoral AT-conditioned medium to mouse monocytes inhibits their proliferation, stimulates phagocytic activity (indicated by increased up-take of adipocyte-derived lipid droplets), and induces morphologic changes characteristic of mature macrophages. Some of these effects on monocytes may be due to direct IL-6 stimulation which is elevated in tumor-associated AT. Similarly, adipocyte-derived endotrophin was recently shown to augment fibrosis, angiogenesis and inflammation by directly recruiting macrophages in a mouse breast tumor model.[28] It is also possible that lipid droplets expelled from damaged tumor-associated adipocytes have a direct effect on macrophage function in tumors. A switch from M2 (anti-inflammatory) into an M1 (pro-inflammatory) macrophage phenotype, characteristic of obese AT, is accompanied by lipid accumulation in ATMs. Based on this finding, the concept of "lipid-induced toxicity" has been coined as the pathogenic link that triggers an inflammatory response in obesity.[29] Indeed, rosiglitazone treatment, which blocks lipid accumulation in macrophages, maintains their M2, anti-inflammatory profile.[30] Surprisingly, Kosteli et al. demonstrated that weight loss is associated with rapid, yet transient recruitment of macrophages into AT. However, in this case, an increase in the number of macrophages does not promote inflammation but rather regulates lipolysis. The authors therefore suggested that release of lipids is a generic signal for macrophage recruitment.[31] As previously described by us and others, the adipose tissue surrounding tumors was characterized by an increase in lipolytic activity. Increased lipid spillage as a result of necrotic death and increased lipolysis within tumor-associated adipose tissue could therefore independently contribute to macrophage recruitment. However, macrophages from tumor-associated adipose tissue expressed markers of both a pro- and anti-inflammatory phenotype suggesting the presence of two distinct populations or that M1 and M2 markers are expressed in a single population. Necrotic adipocyte death could therefore promote recruitment of a pro-inflammatory population exclusively or induce a phenotypic switch in macrophage polarization within a single population.

AT is highly metabolic and dynamically responds to hormonal and nutrient fluctuations and afferent signals from the central nervous system. AT also secretes factors with important endocrine functions, including leptin, adiponectin, multiple cytokines, and growth factors. Thus, dysfunctional adipocytes both in obesity and in tumors could have a profound impact on multiple cell types in the local microenvironment and systemically.[32] These features suggest that adipocytes are central players in the tumor stroma; particularly in those tumors that are closely affiliated with AT (e.g., breast tumors and lymph node metastases). It may be interesting to determine whether some of the same drugs that are currently approved for the treatment of other metabolic syndromes, could also target tumor-associated AT and, as a corollary, control tumor-associated inflammation, tumor growth, and angiogenesis.

Materials and Methods

Mice. Seven- to ten-week-old, sex-matched C57BL/6 and C3H mice were used in all experiments and were purchased from The Jackson Laboratory. All experiments were performed with the approval of the Local Ethical Committee and in accordance with the Norwegian State Commission for Laboratory Animals. Mice were euthanized by CO_2 inhalation.

Cell lines. B16F10 melanoma and M1 mouse myeloid leukemia cells were obtained from the American Type Culture Collection (ATCC). Tumor cells were grown at 37 °C in 5% CO_2 in Dulbecco's modified Eagle's medium (DMEM) supplemented with non-essential amino acids, 10% fetal calf serum, 100 U/ml of penicillin, 100 μg/ml of streptomycin, 400 μM L-glutamine, and Plasmocin™. M1 mouse myeloid leukemia cells were grown at 37 °C in 5% CO_2 in Roswell Park Memorial Institute Medium (RPMI, ACTT) 1640 supplemented with 10% fetal calf serum, 100 U/ml of penicillin, 100 μg/ml of streptomycin, and 400 μM L-glutamine and Plasmocin™.

Tumor cell implantation, peritumoral and control adipose tissue collection. B16F10 melanoma cells (1×10^6) were injected into the anterior, subcutaneous AT depot. When tumors exceeded 2 cm in diameter, animals were euthanized. As described previously by us, peritumoral AT was collected by micro-dissection under a stereoscopic microscope. Control AT from the counterpart depot was collected from age- and sex-matched animals.[14] C3HBA adenocarcinoma and KHT-1 fibrosarcoma tumor tissue samples were a kind gift from Solfrid Johanne Sagstad (Bergen, Norway).

Isolation of SVF population of cells. Freshly harvested samples of control and peritumoral AT were incubated with a mixture of collagenase Type-2 (1 mg/ml), dispase (2.5 μg/ml), and DNase (1 mg/ml) for 1 h at 37 °C with continuous rotation. The dissociated tissue was fractionated by sedimentation centrifugation at 186 g for 10 min. The lipid layer with adipocytes was carefully collected and used for ethidium bromide and acridine orange (EB/AO) staining assay whereas the pelleted stromal vascular fraction was filtered through a 70 μm mesh cell strainer (BD Bioscience) to remove debris. Contaminating erythrocytes were lysed using red blood cell lysis buffer (BD PharMingen). Single cell suspensions were resuspended in RPMI 1640 medium containing 10% fetal calf serum, 100 U/ml of penicillin, 100 μg/ml of streptomycin, and 400 μM L-glutamine and Plasmocin™ and plated on glass coverslips in 24-well plates. This was followed by incubation at 37 °C in a humidified atmosphere of 5% CO_2 in air. After 4 h, nonadherent cells were removed by washing three times with PBS. After 5 d of incubation, the recovered cells were greater than 90% macrophages as analyzed by anti-CD11b staining.

Immunohistochemistry. Tissue samples were fixed in 4% PFA, paraffin-embedded, and cut into 4 μm sections. For

immunolabeling, sections were deparaffinized and rehydrated before antigen retrieval at 98 °C for 1 h in 0.01 M citrate buffer (pH 6.0). After blocking with diluted serum from the secondary antibody host for 30 min, the slides were incubated overnight (4 °C) with the primary antibody. After blocking endogenous peroxidase activity for 20 min with 3% hydrogen peroxide, a biotinylated anti-rat or anti-rabbit secondary antibody (Vector Laboratories) was applied for 45 min as appropriate. The antigen-antibody complex reaction was augmented with avidin-biotin-peroxidase (ABC) for 45 min according to the manufacturer's instructions (Vectastain® ABC Kit, Vector), and stained for 1–10 min with diamino-benzidine tetrahydrochloride (DAB, Vector). The sections were then counterstained with hematoxylin (Fisher), dehydrated and mounted with Entellan (Electron Microscopy Services). Parallel sections were run for all the experiments without primary antibody to assure the specificity of the immunoreactions. Primary antibodies were as followed: rabbit anti-perilipin-1 (1:200; Cell Signaling), rabbit anti-HMGB1 (1:200; Abcam), and rabbit anti-IL-6 (1:100; Abcam).

Ethidium bromide and acridine orange (EB/AO) staining assay. Adipocytes were stained with acridine orange (AO) (100 μg/ml, Sigma) and ethidium bromide (100 μg/ml, EB) (Sigma) dye mix according to procedure of Ribble et al.[33] Briefly, freshly isolated adipocytes were re-suspended in 25 μl cold PBS and 2 μl EB/AO dye mix was added. The stained cell suspension (10 μl) was placed on a clean microscope slide and covered with a coverslip. Cells were viewed and counted using a Nikon Eclipse e600 microscope at 100× magnification. Experiments were done in triplicate, counting a minimum of 100 total cells each.

Transmission electron microscopy. AT pieces (about 1-mm cubed) were fixed in 2.5% glutaraldehyde (diluted in 0.1 M Na-cacodylate buffer) and post-fixed in 1% osmium tetroxide (OsO_4) (diluted in 0.1 M Na-cacodylate buffer). The pieces were then embedded in epoxy resin Agar 100 and sliced into 60 nm thick sections. Next sections were stained with lead-citrate and uranyl-acetate before examination with a transmission electron microscope (JEM-1230, Jeol). Representative photomicrographs were selected for analysis.

Western blot. Tissue samples were homogenized and cells were sonicated in a custom made total protein lysis buffer (50 mM TRIS-HCl, pH 7.5, 150 mM NaCl, 0.1% SDS, 1% deoxycholate, 1% Triton X-100) containing a protease and phosphatase inhibitor cocktail (Roche). Protein concentrations were measured using bicinchoninic acid (BCA) assay (Pierce), and 30 μg protein was loaded per lane for all the immunoblots. The protein lysates were fractionated using NuPAGE Novex 4–12% Bis-Tris Gel (Invitrogen) elecrophoresis and transblotted to nitrocellulose membranes using the XCell II Blot Module (Invitrogen). Protein transfer was assessed by Ponseau S solution (Sigma Aldrich). Next membranes were blocked with 5% fat-free dry milk for 1 h before immunoblotting overnight with the primary antibody. The immobilized antibody was detected using the appropriate horseradish peroxidase-conjugated secondary antibody and SuperSignal West Pico Chemiluminescent Substrate (Thermo Scientific). The immune reaction was visualized using a LAS-3000 imaging system (FujiFilm). Immunoblots for β-actin were performed to assure equal protein loading. Primary antibodies were as follow: rabbit anti-perilipin-1 (1:1000; Cell Signaling), rat anti-CD301 (1:500; AbD Serotec), and rabbit anti-β actin (1:200; Abcam). Secondary antibodies were as follows: anti-rat IgG-Peroxidase (1:80000; Sigma Aldrich) and anti-rabbit IgG-Peroxidase (1:20000; Beckman Coulter).

Preparation of conditioned media. AT-conditioned medium was prepared from peritumoral ($n = 3$) and control AT ($n = 3$) normalized to 0.5 g. Twenty-four hours after medium replacement, conditioned medium was aspirated and filtered through a 0.22 μm membrane (Millipore) and stored at –80 °C.

Oil-red-O staining. Cells were fixed in 4% paraformaldehyde for 10 min, stained with Oil-red-O (Sigma Aldrich) for 15 min, and then stained with hematoxylin for 3 min. Cells were washed three times with ddH_2O and examined by light microscopy. The intracellular lipid droplets were stained red, and cell nuclei were stained blue.

ELISA. The IL-6 ELISA was purchased from R&D Systems. ELISA was performed as recommended by the distributor. For the determination of IL-6, both peritumoral and control AT-conditioned media were diluted 10-fold and measurements were done in duplicate.

M1 myeloid cell viability assay. M1 cells were seeded into a 96-well microtiter plate at a final density of 2.5×10^3 cells/well in 100 μl of AT-conditioned medium or medium supplemented with different concentrations of IL-6 (R&D Systems). Cells were then treated with 20 μl of a solution comprising 1.9 mg/mL of MTS [3-(4,5-dimethylthiazol-2-yl)-5-(3-carboxymethoxyphenyl)-2-(4-sulfophenyl)-2 tetrazolium, inner salt; MTS] in phosphate-buffered saline (PBS) pH 6.0. The plate was then incubated for an additional 1 h. The absorbance of the soluble formazan salt was measured against a tetrazolium standard MTS solution. The experiment was done in triplicate.

Macrophage differentiation assay. M1 myeloid cells were seeded at a density of 2.5×10^5/ml into 24-well culture plates with glass coverslips. After five days, the non-adherent cells were removed by washing with PBS and attached cells were fixed with 4% paraformaldehyde. Differentiation was assessed in triplicate by counting the number of cells attached to coverslips in three independent fields.

Statistics. In all experiments, the statistical significance was analyzed by the unpaired Student t test using Prism software (GraphPad, Inc.). The value of $P < 0.05$ was considered statistically significant.

Disclosure of Potential Conflicts of Interest

No potential conflicts of interest were disclosed.

Acknowledgments

References

1. Andarawewa KL, Motrescu ER, Chenard MP, Gansmuller A, Stoll I, Tomasetto C, et al. Stromelysin-3 is a potent negative regulator of adipogenesis participating to cancer cell-adipocyte interaction/crosstalk at the tumor invasive front. Cancer Res 2005; 65:10862-71; PMID:16322233; http://dx.doi.org/10.1158/0008-5472.CAN-05-1231

2. Tan JX, Buache E, Chenard MP, Dali-Youcef N, Rio MC. Adipocyte is a non-trivial, dynamic partner of breast cancer cells. Int J Dev Biol 2011; 55:851-9; PMID:21948738; http://dx.doi.org/10.1387/ijdb.113365jt

3. Rio MC. The Role of Cancer-Associated Adipocytes (CAA) in the Dynamic Interaction Between the Tumor and the Host. Springer Netherlands, 2011.

4. Bochet L, Meulle A, Imbert S, Salles B, Valet P, Muller C. Cancer-associated adipocytes promotes breast tumor radioresistance. Biochem Biophys Res Commun 2011; 411:102-6; PMID:21712027; http://dx.doi.org/10.1016/j.bbrc.2011.06.101

5. Behan JW, Yun JP, Proektor MP, Ehsanipour EA, Arutyunyan A, Moses AS, et al. Adipocytes impair leukemia treatment in mice. Cancer Res 2009; 69:7867-74; PMID:19773440; http://dx.doi.org/10.1158/0008-5472.CAN-09-0800

6. Kushiro K, Chu RA, Verma A, Núñez NP. Adipocytes Promote B16BL6 Melanoma Cell Invasion and the Epithelial-to-Mesenchymal Transition. Cancer Microenviron 2012; 5:73-82; PMID:21892698; http://dx.doi.org/10.1007/s12307-011-0087-2

7. Dirat B, Bochet L, Dabek M, Daviaud D, Dauvillier S, Majed B, et al. Cancer-associated adipocytes exhibit an activated phenotype and contribute to breast cancer invasion. Cancer Res 2011; 71:2455-65; PMID:21459803; http://dx.doi.org/10.1158/0008-5472.CAN-10-3323

8. Nieman KM, Kenny HA, Penicka CV, Ladanyi A, Buell-Gutbrod R, Zillhardt MR, et al. Adipocytes promote ovarian cancer metastasis and provide energy for rapid tumor growth. Nat Med 2011; 17:1498-503; PMID:22037646; http://dx.doi.org/10.1038/nm.2492

9. Schipper HS, Prakken B, Kalkhoven E, Boes M. Adipose tissue-resident immune cells: key players in immunometabolism. Trends Endocrinol Metab 2012; 23:407-15; PMID:22795937; http://dx.doi.org/10.1016/j.tem.2012.05.011

10. Lotze MT, Tracey KJ. High-mobility group box 1 protein (HMGB1): nuclear weapon in the immune arsenal. Nat Rev Immunol 2005; 5:331-42; PMID:15803152; http://dx.doi.org/10.1038/nri1594

11. Rock KL, Kono H. The inflammatory response to cell death. Annu Rev Pathol 2008; 3:99-126; PMID:18039143; http://dx.doi.org/10.1146/annurev.pathmechdis.3.121806.151456

12. Schrijvers DM, De Meyer GR, Kockx MM, Herman AG, Martinet W. Phagocytosis of apoptotic cells by macrophages is impaired in atherosclerosis. Arterioscler Thromb Vasc Biol 2005; 25:1256-61; PMID:15831805; http://dx.doi.org/10.1161/01.ATV.0000166517.18801.a7

13. Qian BZ, Pollard JW. Macrophage diversity enhances tumor progression and metastasis. Cell 2010; 141:39-51; PMID:20371344; http://dx.doi.org/10.1016/j.cell.2010.03.014

14. Wagner M, Bjerkvig R, Wiig H, Melero-Martin JM, Lin RZ, Klagsbrun M, et al. Inflamed tumor-associated adipose tissue is a depot for macrophages that stimulate tumor growth and angiogenesis. Angiogenesis 2012; 15:481-95; PMID:22614697; http://dx.doi.org/10.1007/s10456-012-9276-y

15. Wagner M, Dudley AC. A three-party alliance in solid tumors: Adipocytes, macrophages and vascular endothelial cells. Adipocyte 2013; 2:67-73; http://dx.doi.org/10.4161/adip.23016

16. Scaffidi P, Misteli T, Bianchi ME. Release of chromatin protein HMGB1 by necrotic cells triggers inflammation. Nature 2002; 418:191-5; PMID:12110890; http://dx.doi.org/10.1038/nature00858

17. Bianchi ME, Manfredi AA. Immunology. Dangers in and out. Science 2009; 323:1683-4; PMID:19325105; http://dx.doi.org/10.1126/science.1172794

18. Andersson U, Wang H, Palmblad K, Aveberger AC, Bloom O, Erlandsson-Harris H, et al. High mobility group 1 protein (HMG-1) stimulates proinflammatory cytokine synthesis in human monocytes. J Exp Med 2000; 192:565-70; PMID:10952726; http://dx.doi.org/10.1084/jem.192.4.565

19. Cinti S, Mitchell G, Barbatelli G, Murano I, Ceresi E, Faloia E, et al. Adipocyte death defines macrophage localization and function in adipose tissue of obese mice and humans. J Lipid Res 2005; 46:2347-55; PMID:16150820; http://dx.doi.org/10.1194/jlr.M500294-JLR200

20. Paul A, Chang BH, Li L, Yechoor VK, Chan L. Deficiency of adipose differentiation-related protein impairs foam cell formation and protects against atherosclerosis. Circ Res 2008; 102:1492-501; PMID:18483409; http://dx.doi.org/10.1161/CIRCRESAHA.107.168070

21. Grivennikov SI, Greten FR, Karin M. Immunity, inflammation, and cancer. Cell 2010; 140:883-99; PMID:20303878; http://dx.doi.org/10.1016/j.cell.2010.01.025

22. Matzinger P. The danger model: a renewed sense of self. Science 2002; 296:301-5; PMID:11951032; http://dx.doi.org/10.1126/science.1071059

23. Wang HC, Bloom O, Zhang MH, Vishnubhakat JM, Ombrellino M, Che JT, et al. HMG-1 as a late mediator of endotoxin lethality in mice. Science 1999; 285:248-51; PMID:10398600; http://dx.doi.org/10.1126/science.285.5425.248

24. Gardella S, Andrei C, Ferrera D, Lotti LV, Torrisi MR, Bianchi ME, et al. The nuclear protein HMGB1 is secreted by monocytes via a non-classical, vesicle-mediated secretory pathway. EMBO Rep 2002; 3:995-1001; PMID:12231511; http://dx.doi.org/10.1093/embo-reports/kvf198

25. Kalluri R, Zeisberg M. Fibroblasts in cancer. Nat Rev Cancer 2006; 6:392-401; PMID:16572188; http://dx.doi.org/10.1038/nrc1877

26. Pollard JW. Tumour-educated macrophages promote tumour progression and metastasis. Nat Rev Cancer 2004; 4:71-8; PMID:14708027; http://dx.doi.org/10.1038/nrc1256

27. Condeelis J, Pollard JW. Macrophages: obligate partners for tumor cell migration, invasion, and metastasis. Cell 2006; 124:263-6; PMID:16439202; http://dx.doi.org/10.1016/j.cell.2006.01.007

28. Park J, Scherer PE. Adipocyte-derived endotrophin promotes malignant tumor progression. J Clin Invest 2012; 122:4243-56; PMID:23041627; http://dx.doi.org/10.1172/JCI63930

29. Prieur X, Roszer T, Ricote M. Lipotoxicity in macrophages: evidence from diseases associated with the metabolic syndrome. Biochim Biophys Acta 2010; 1801:327-37; PMID:19796705; http://dx.doi.org/10.1016/j.bbalip.2009.09.017

30. Prieur X, Mok CYL, Velagapudi VR, Núñez V, Fuentes L, Montaner D, et al. Differential lipid partitioning between adipocytes and tissue macrophages modulates macrophage lipotoxicity and M2/M1 polarization in obese mice. Diabetes 2011; 60:797-809; PMID:21266330; http://dx.doi.org/10.2337/db10-0705

31. Kosteli A, Sugaru E, Haemmerle G, Martin JF, Lei J, Zechner R, et al. Weight loss and lipolysis promote a dynamic immune response in murine adipose tissue. J Clin Invest 2010; 120:3466-79; PMID:20877011; http://dx.doi.org/10.1172/JCI42845

32. Attie AD, Scherer PE. Adipocyte metabolism and obesity. J Lipid Res 2009; 50(Suppl):S395-9; PMID:19017614; http://dx.doi.org/10.1194/jlr.R800057-JLR200

33. Ribble D, Goldstein NB, Norris DA, Shellman YG. A simple technique for quantifying apoptosis in 96-well plates. BMC Biotechnol 2005; 5:12; PMID:15885144; http://dx.doi.org/10.1186/1472-6750-5-12